

Search for New Particles Decaying to Dijets, $b\bar{b}$, and $t\bar{t}$ at CDF

CDF Collaboration

Presented by
 Robert M. Harris

*Fermilab MS 318
 Batavia, IL 60510*

We present three searches for new particles at CDF. First, using 70 pb^{-1} of data we search the dijet mass spectrum for resonances. There is an upward fluctuation near $550 \text{ GeV}/c^2$ (2.6σ) with an angular distribution that is adequately described by either QCD alone or QCD plus 5% signal. There is insufficient evidence to claim a signal, but we set the most stringent mass limits on the hadronic decays of axigluons, excited quarks, technirhos, W' , Z' , and E_6 diquarks. Second, using 19 pb^{-1} of data we search the b-tagged dijet mass spectrum for $b\bar{b}$ resonances. Again, an upward fluctuation near $600 \text{ GeV}/c^2$ (2σ) is not significant enough to claim a signal, so we set the first mass limits on topcolor bosons. Finally, using 67 pb^{-1} of data we search the top quark sample for $t\bar{t}$ resonances like a topcolor Z' . Other than an insignificant shoulder of 6 events on a background of 2.4 in the mass region $475\text{-}550 \text{ GeV}/c^2$, there is no evidence for new particle production. Mass limits, currently in progress, should be sensitive to a topcolor Z' near $600 \text{ GeV}/c^2$. In all three searches there is insufficient evidence to claim new particle production, yet there is an exciting possibility that the upward fluctuations are the first signs of new physics beyond the standard model.

I. SEARCH FOR NEW PARTICLES DECAYING TO DIJETS

As in our previous analysis of Run 1A data (1), we conduct a general search for new particles with a narrow natural width that decay to dijets. In addition, we search for the following particles summarized in Fig. 1: axigluons (2) from chiral QCD ($A \rightarrow q\bar{q}$), excited states (3) of composite quarks ($q^* \rightarrow qg$), color octet technirhos (4) ($\rho_T \rightarrow g \rightarrow q\bar{q}, gg$), new gauge bosons ($W', Z' \rightarrow q\bar{q}$), and scalar E_6 diquarks (5) ($D \rightarrow \bar{u}\bar{d}$ and $D^c \rightarrow ud$).

Using four triggers from run 1A and 1B, we combine dijet mass spectra above a mass of $150 \text{ GeV}/c^2$, $241 \text{ GeV}/c^2$, $292 \text{ GeV}/c^2$, and $388 \text{ GeV}/c^2$ with integrated luminosities of

New Particles that Decay to Dijets

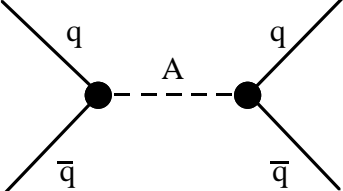
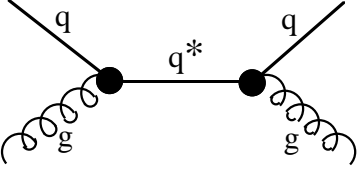
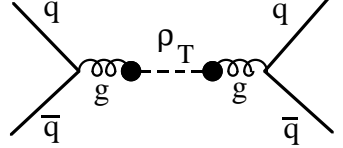
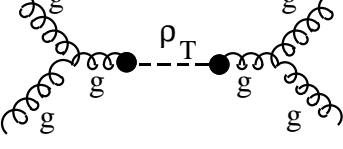
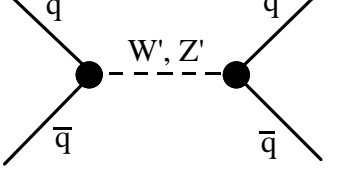
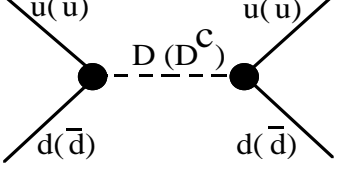
<u>Model</u>	<u>Particle</u>	<u>Production/Decay</u>	$J^P(\text{color})$ <u>& $\Gamma/2$</u>	<u>Reference &</u> <u>$\sigma_B(500 \text{ GeV})$</u>
Chiral Color $SU(3)_L \times SU(3)_R$	Axigluon A		$1^+(8)$.05M	Bagger, Schmidt & King.1988 210 pb
Composite Fermions	Excited Quark q^*		$1/2^+(3)$.02M	Baur, Hinchliffe & Zeppenfeld 1987 40 pb
Technicolor	Technirho ρ_T		$1^-(8)$	Eichten & Lane 1994
			.01M	Lane & Ramana 1991 13 pb
Extended Gauge Models. $SU(2)_L \times SU(2)_R$ E_6 , etc	New Gauge Bosons W', Z'		$1(1)$.01M	Standard Model Couplings 5 pb, 4 pb
Superstring Inspired E_6 Models	Diquarks D, D^C		$0^+(\bar{3})$.004M	Hewett & Rizzo 1989 4 pb

FIG. 1. For each new particle that decays to dijets we list the model name, the particle name, the Feynman diagram, and a 2×2 text grid containing the quantum numbers, a reference, the half-width and the cross section at a mass of $500 \text{ GeV}/c^2$. The production and decay couplings for the first three particles are strong, for new gauge bosons the coupling is weak, and for E_6 diquarks the coupling is electromagnetic.

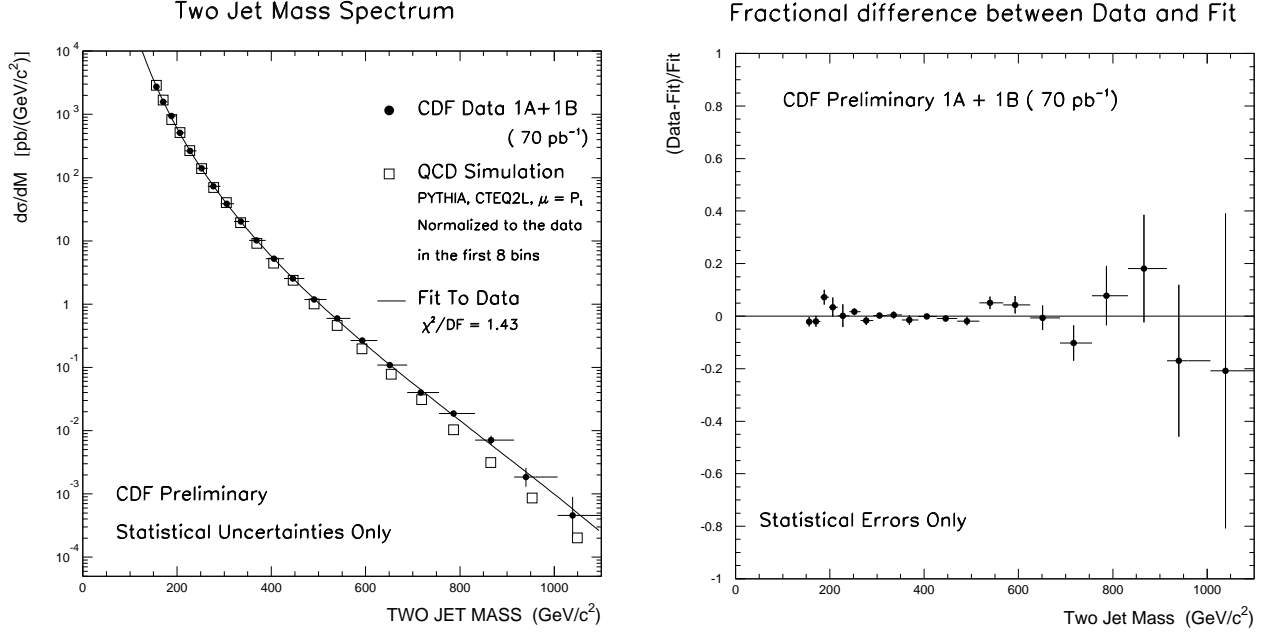


FIG. 2. The dijet mass data (solid points) is compared to a parameterization fit to the data (curve). The logarithmic plot also shows a QCD simulation (open boxes).

.089 pb⁻¹, 1.92 pb⁻¹, 9.52 pb⁻¹, and 69.8 pb⁻¹ respectively. Jets are defined with a fixed cone clustering algorithm ($R=0.7$) and then corrected for detector response, energy lost outside the cone, and underlying event. We take the two highest P_T jets and require that they have pseudorapidity $|\eta| < 2$ and a CMS scattering angle $|\cos\theta^*| = |\tanh[(\eta_1 - \eta_2)/2]| < 2/3$. The $\cos\theta^*$ cut provides uniform acceptance as a function of mass and reduces the QCD background which peaks at $|\cos\theta^*| = 1$. In Fig. 2 the dijet mass distribution is presented as a differential cross section in bins of the mass resolution ($\sigma \sim 10\%$). At high mass the data is systematically higher than a prediction from PYTHIA plus a CDF detector simulation, similar to the inclusive jet E_T spectrum (6). To search for new particles we determine the QCD background by fitting the data to a smooth function of three parameters (7); Fig. 2 shows the fractional difference between the data and the fit ($\chi^2/DF = 1.43$). We note upward fluctuations near 200 GeV/c² (2.4σ), 550 GeV/c² (2.6σ) and 850 GeV/c² (1σ).

For narrow resonances it is sufficient to determine the mass resolution for only one type of new particle because the detector resolution dominates the width. In Fig. 3 we show the mass resolution for excited quarks (q^*) from PYTHIA plus a CDF detector simulation; the long tail at low mass comes from gluon radiation. For each value of new particle mass in 50 GeV/c² steps, we perform a binned maximum likelihood fit of the data to the background parameterization and the mass resonance shape. In Fig. 3 we display the best fit and 95% confidence level upper limit for a 550 GeV/c² resonance. For the mass region $517 < M < 625$ GeV/c², there are 2947 events in the data, 2810 ± 53 events (2.6σ) in the background for the fit without a resonance, 2765 ± 53 events (3.4σ) in the background for the fit that includes the resonance, and the value of the resonance cross section from the fit is 5.8 ± 2.9 pb (statistical).

In Fig. 4 we study the angular distribution of the fluctuation in the mass region $517 < M < 625$ GeV/c². The angular distribution is compatible with both QCD alone, and with

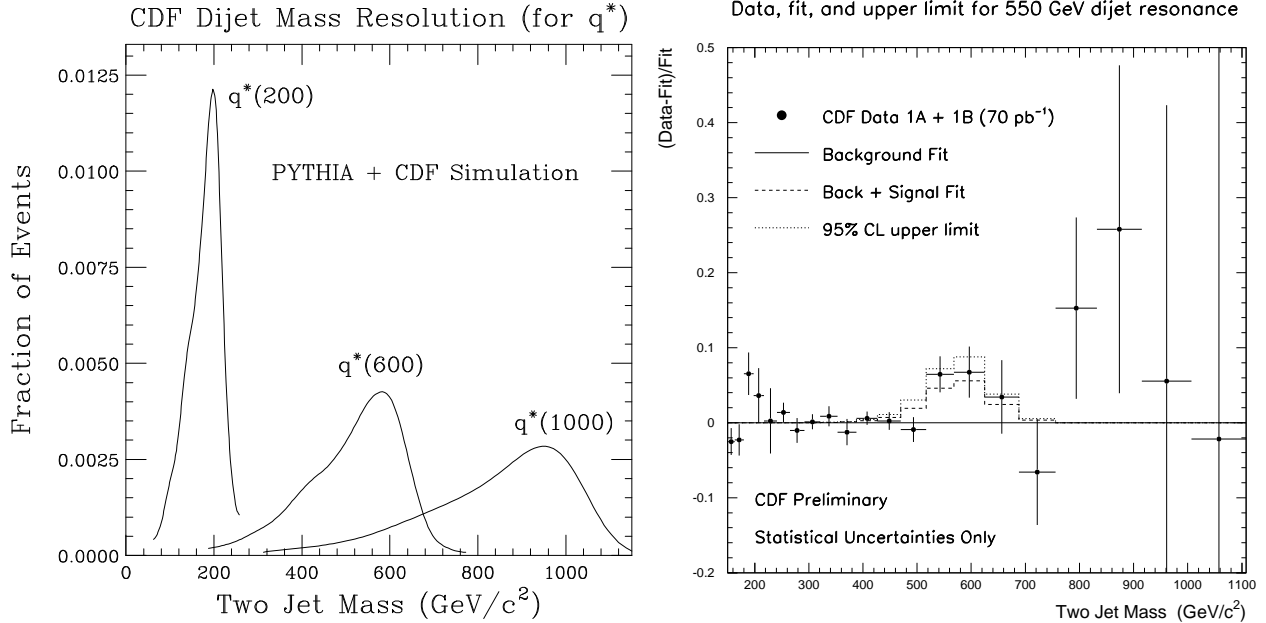


FIG. 3. left: CDF dijet mass resolution for narrow resonances like excited quarks, including the effects of radiation and detector resolution. right: The dijet mass data (solid points) fit with a background (solid line) and a $550 \text{ GeV}/c^2$ resonance (dashed hist).

QCD + 5% excited quark (best fit). This amount of excited quark is coincidentally the same as found in the mass fit. Although the fluctuation is interesting, we conclude it is not yet statistically significant, and proceed to set limits on new particle production.

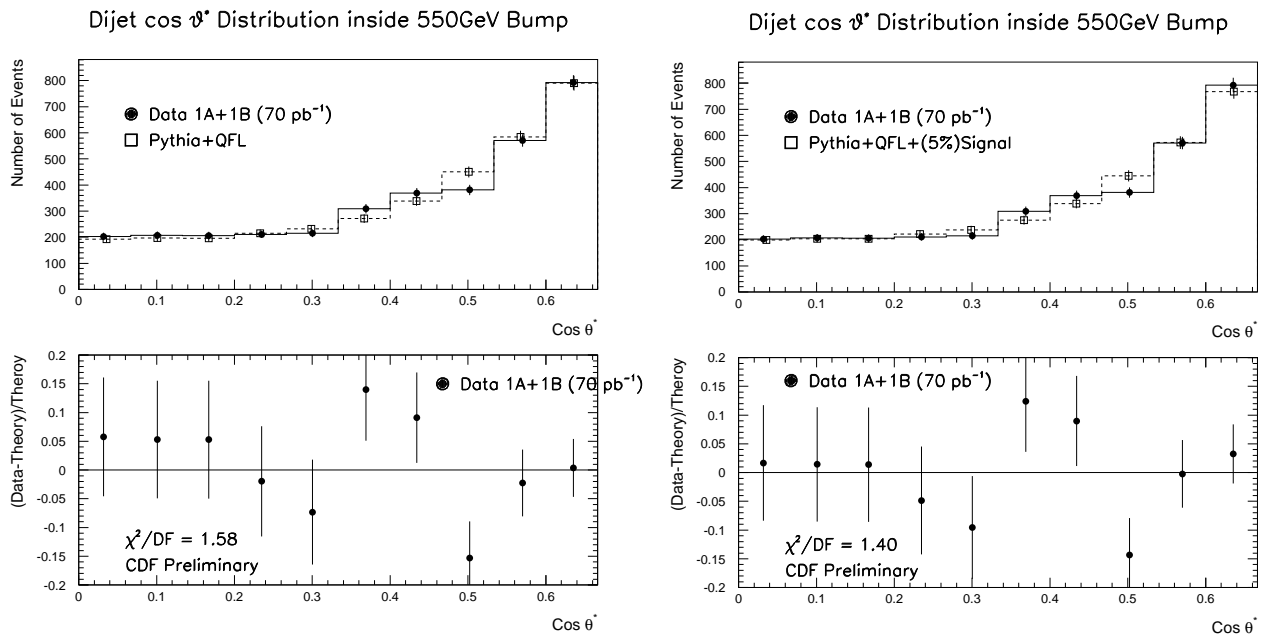


FIG. 4. left: The angular distribution of data in the two central bins of the $550 \text{ GeV}/c^2$ fluctuation (solid points) is compared to a QCD simulation (open boxes) and the fractional difference is shown beneath. right: same as left but fit to a QCD simulation plus a floating signal. The predictions are normalized to the data.

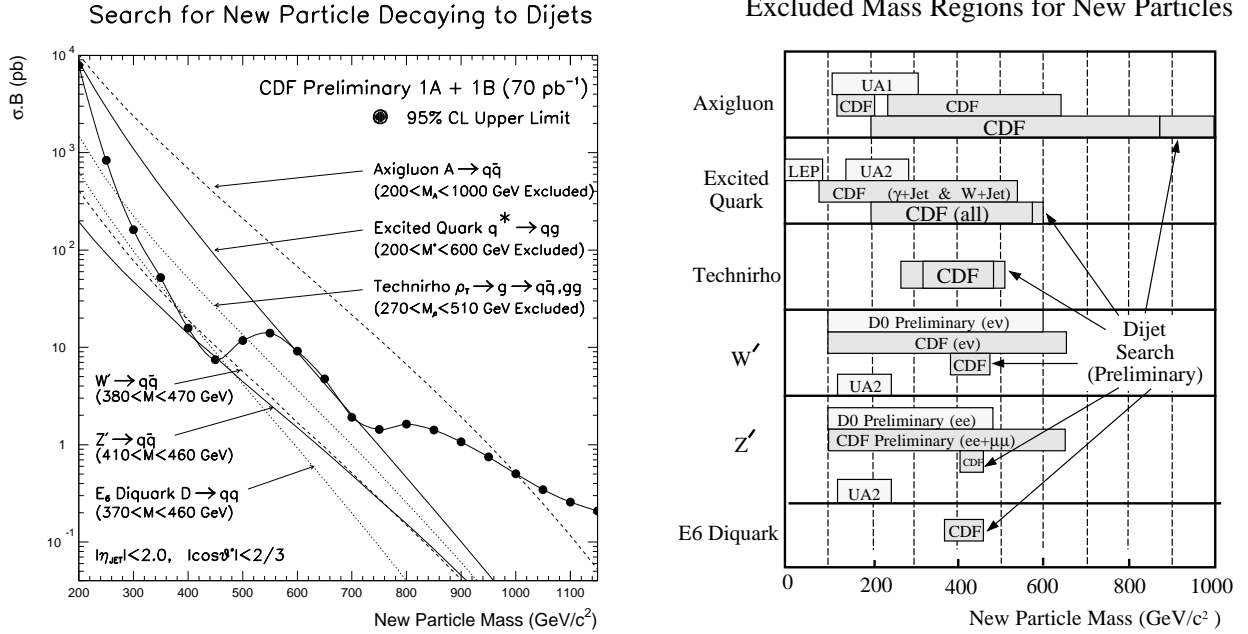


FIG. 5. left: Upper limits on the cross section for new particles. right: Excluded mass regions compared to previous searches.

From the likelihood distribution including experimental systematic uncertainties (1) we obtain the 95% CL upper limit on the cross section for new particles shown in Fig. 5. We compare this to the cross section for axigluons (excluding $200 < M < 1000 \text{ GeV}/c^2$), excited quarks (excluding $200 < M < 600 \text{ GeV}/c^2$), technirhos (excluding $270 < M < 510 \text{ GeV}/c^2$), W' (excluding $380 < M < 470 \text{ GeV}/c^2$), Z' (excluding $410 < M < 460 \text{ GeV}/c^2$), and E_6 diquarks (excluding $370 < M < 460 \text{ GeV}/c^2$). The calculations are lowest order (8) using CTEQ2L parton distributions (9) and one-loop $\alpha_s(m^2)$ and require $|\eta| < 2$ and $|\cos\theta^*| < 2/3$.

II. TOPCOLOR

The large mass of the top quark suggests that the third generation may be special. Topcolor (10,11) assumes that the top mass is large mainly because of a dynamical $t\bar{t}$ condensate generated by a new strong dynamics coupling to the third generation. Here the $SU(3)_C$ of QCD is a low energy symmetry arising from the breaking of an $SU(3)_1$ coupling to the third generation and an $SU(3)_2$ coupling to the first two generations only. There are then massive color octet bosons, topgluons B , which couple largely to $b\bar{b}$ and $t\bar{t}$. The topgluon is strongly produced and decays mainly to the third generation ($q\bar{q} \rightarrow B \rightarrow b\bar{b}, t\bar{t}$) with a relatively large natural width ($\Gamma \geq 0.11M$). Here we search for the topgluon in the $b\bar{b}$ channel.

An additional $U(1)$ symmetry is introduced (11) to keep the b quark light while the top quark is heavy; this leads to a topcolor Z' , which again couples largely to $b\bar{b}$ and $t\bar{t}$. The topcolor Z' is electroweakly produced and decays mainly to the third generation ($q\bar{q} \rightarrow Z' \rightarrow b\bar{b}, t\bar{t}$) with a narrow natural width ($\Gamma \geq 0.012M$). Here we search for the topcolor Z' in both the $b\bar{b}$ and $t\bar{t}$ channel; the $t\bar{t}$ channel is the most sensitive because the coupling to $t\bar{t}$ is larger.

III. SEARCH FOR NEW PARTICLES DECAYING TO $B\bar{B}$

We start with the dijet search in 19 pb^{-1} of run 1A data (1) and additionally require at least one of the two leading jets be tagged as a bottom quark. The b-tag requires a displaced vertex in the the secondary vertex detector (12). The $b\bar{b}$ event efficiency is $25 \pm 2\%$ independent of dijet mass. From fits to the $c\tau$ distribution, we estimate that the sample is roughly 50% bottom, 30% charm, and 20% mistags of plain jets. PYTHIA predicts that 1/5 of these bottom quarks are direct $b\bar{b}$, and the rest are from gluon splitting and flavor excitation. Consequentially, only about $1/5 \times 50\% = 10\%$ of our sample is direct $b\bar{b}$. We expect both the purity and efficiency to increase when we use the run 1B dataset and a new tagging algorithm (13). With higher tagging efficiency we should be able to make better use of double b-tagged events like the one in Fig. 6.

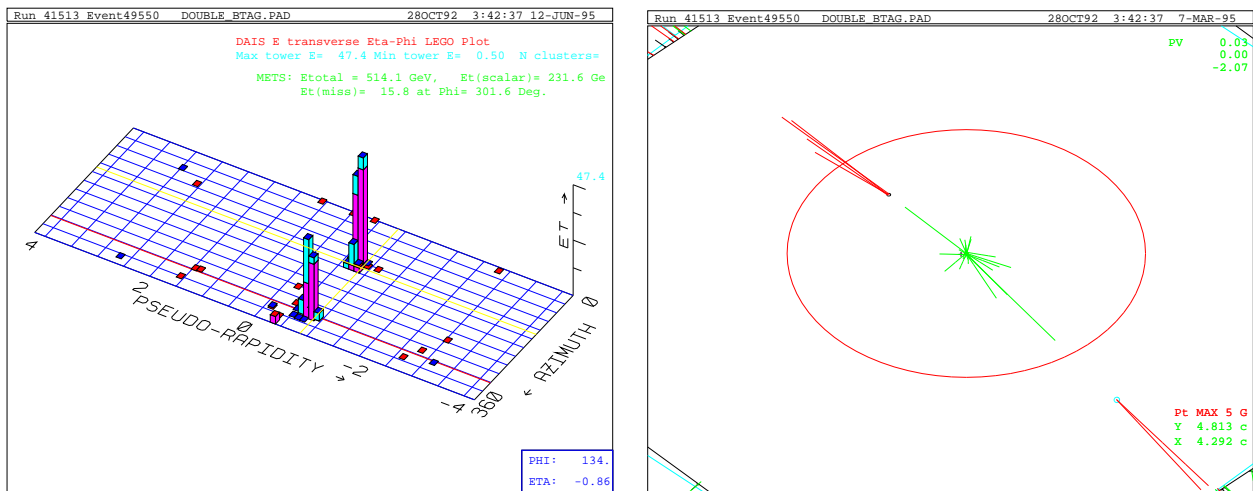


FIG. 6. The highest mass ($256 \text{ GeV}/c^2$) double b-tagged dijet event. left: Lego plot showing the two jets. right: Vertex plot showing the SVX tracks forming displaced secondary vertices: one inside the beam pipe, the other outside.

In Fig. 7 we show the b-tagged dijet mass distribution corrected for the $b\bar{b}$ efficiency. Also shown is the untagged dijet mass distribution from run 1A, and both are well fit with our standard parameterization (7). The b-tagged dijet data has an upward fluctuation near $600 \text{ GeV}/c^2$. We model the shape of a narrow resonance using PYTHIA Z' production and a CDF detector simulation. In Fig. 7 we fit the b-tagged data to a $600 \text{ GeV}/c^2$ narrow resonance, and find a cross section of $3.2 \pm 1.6 \text{ pb}$ (statistical). Note that this is comparable to the dijet fluctuation in both mass and rate. However, there are only 8 events in the last two data bins of Fig. 7, and the fluctuation is only a 2σ effect, so we proceed to set limits on new particle production.

We perform two kinds of fits for the limits. First, narrow resonances are modelled as described above, and the mass resolution in the CDF detector is shown in Fig. 8. Second, wide resonances characteristic of topgluons (14), including interference with normal gluons, was incorporated into PYTHIA and a CDF detector simulation. The mass resolution in Fig. 8 displays destructive interference to the left of the resonance; models with destructive interference on the right side of the resonance will be considered in the future.

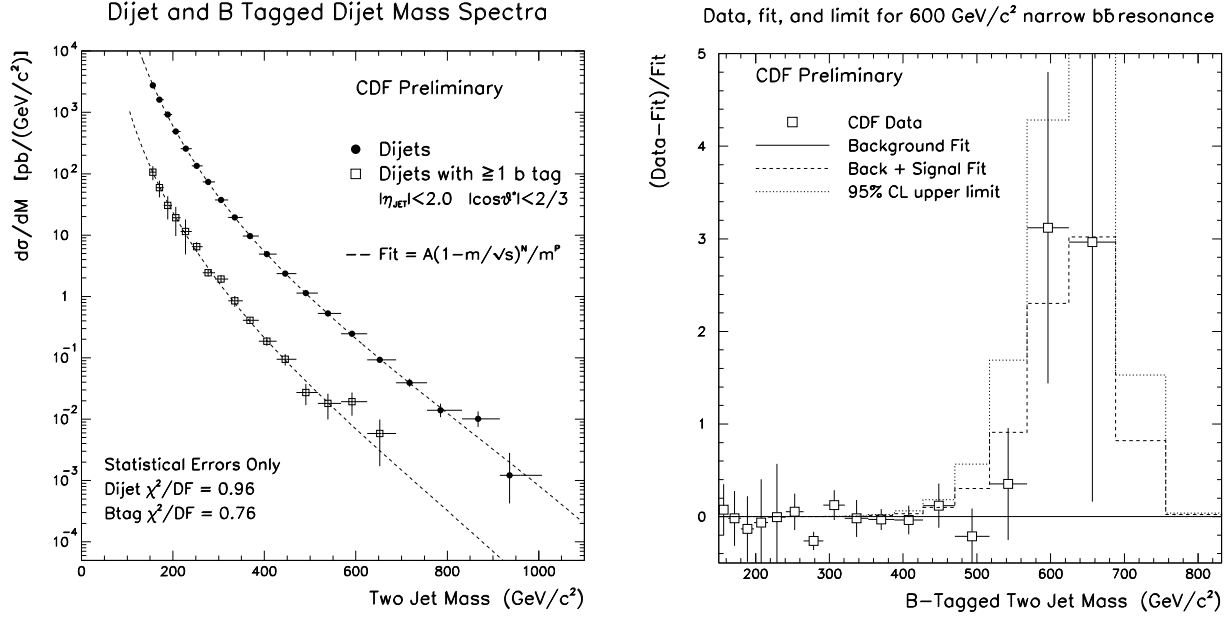


FIG. 7. left: Dijet mass data (solid points) and b-tagged dijet mass data (open boxes) both from run 1A only, are compared to a parameterization fit to the data (curve). right: The b-tagged dijet mass data (open boxes) fit by a background (solid line) and a 600 GeV/c² narrow resonance (dashed hist).

Limits on new particle production are shown in Fig. 9. The theoretical cross sections are lowest order and use CTEQ2L parton distributions. For narrow resonances the production cross sections aren't large enough for us to set mass limits at this time. For topgluons the production cross sections (15) are larger, and we are able to exclude at 95% CL topgluons of width $\Gamma = 0.11M$ in the mass region $200 < M < 550$ GeV/c², $\Gamma = 0.3M$ for $210 < M < 450$ GeV/c², and $\Gamma = 0.5M$ for $200 < M < 370$ GeV/c².

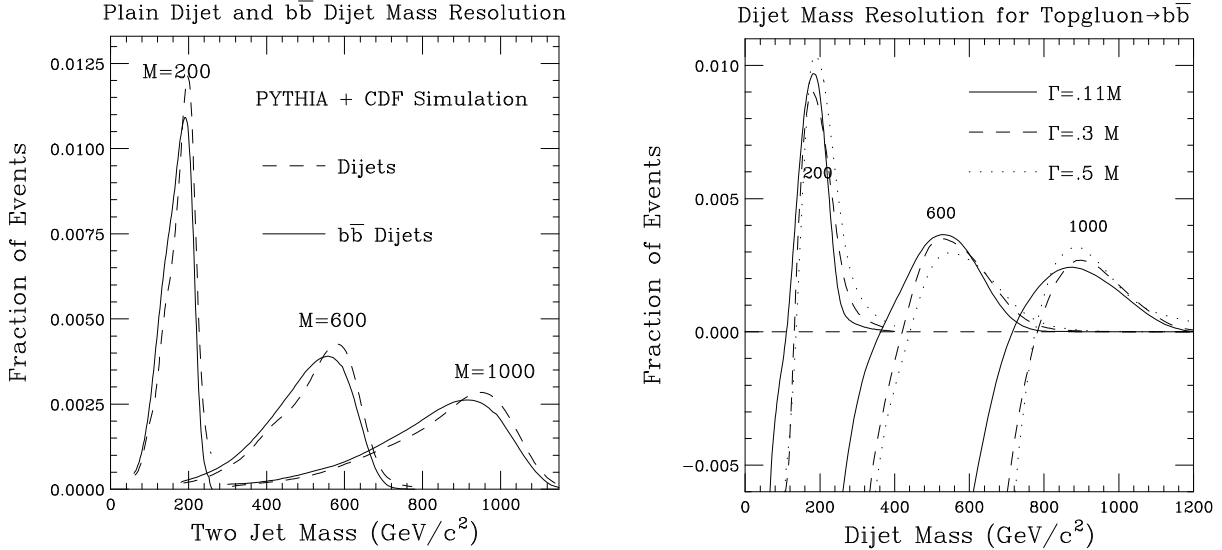


FIG. 8. left: $b\bar{b}$ mass resolution for narrow resonances like topcolor Z' , including the effects of radiation and detector resolution. right: $b\bar{b}$ mass resolution for topgluons, including interference with $g \rightarrow b\bar{b}$, are shown for three different topgluon widths.

Search for New Particles decaying to $b\bar{b}$ with b -tagged dijets

(CDF Preliminary, Stat Uncertainties Only, $|\eta_{jet}| < 2$, $|\cos\theta^*| < 2/3$)

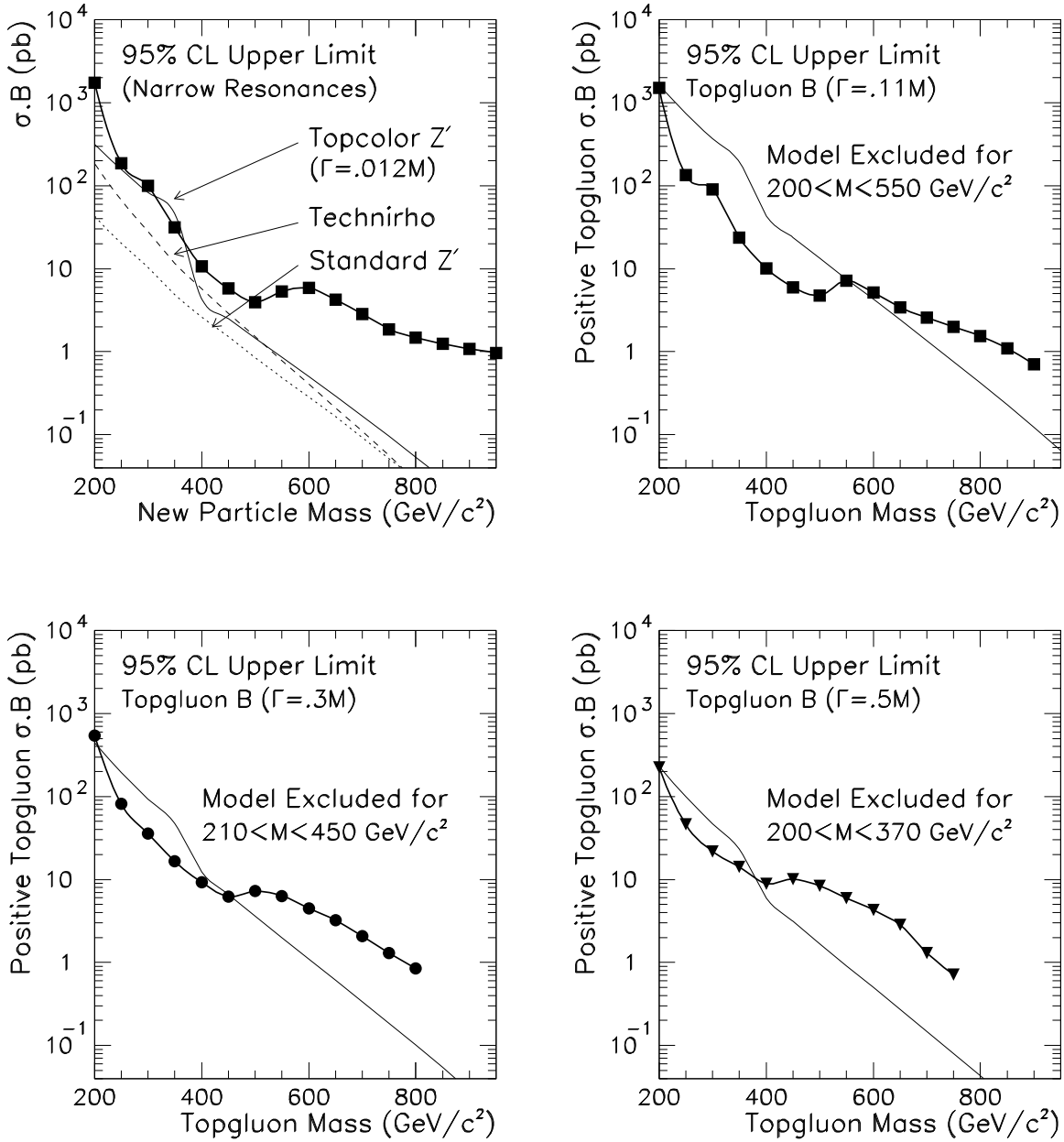


FIG. 9. upper left: Preliminary upper limits on the cross section for a narrow resonances decaying to $b\bar{b}$ (squares) are compared to the theoretical prediction for topcolor Z' , color octet technirhos, and a standard Z' . remaining plots: Upper limits on cross section for topcolor bosons of fractional width 0.11 (squares), 0.3 (circles) and 0.5 (triangles) are compared with theoretical predictions for topgluons; excluded mass regions are listed. What is plotted is the positive topgluon cross section and limits: the cross section in that region where the topgluon produces an excess above QCD (there is a region where the destructive interference between the topgluon and the normal gluon drives the total cross section beneath the standard QCD prediction; see fig. 8).

IV. SEARCH FOR NEW PARTICLES DECAYING TO $t\bar{t}$

To search for new particles decaying to $t\bar{t}$ we start with the data sample from the top mass measurement (13). There we used top decays to $W + \text{four jets}$ with at least one b-tag, and found 19 events on a background of $\sim 7 \pm 2$, resulting in a top mass of $176 \pm 8(\text{stat}) \pm 10(\text{sys}) \text{ GeV}/c^2$. That analysis fit the entire event for the top hypothesis, discarding events with $\chi^2 > 10$ (poor fit). Here we add the additional constraint that the top mass is $176 \text{ GeV}/c^2$, which significantly enhances our resolution of the $t\bar{t}$ mass. Two of the 19 events fail the $\chi^2 > 10$ cut when the top mass constraint is added to the fit, leaving us with 17 events.

The $t\bar{t}$ mass distribution expected from a narrow resonance, normalized to the topcolor Z' predicted rate (15), is shown in Fig. 10. Here we used PYTHIA $Z' \rightarrow t\bar{t}$. Also in Fig. 10 is the Monte Carlo distribution of the background, on the left standard model top production from HERWIG, and on the right QCD $W + \text{jets}$ background from VECBOS with parton showers from HERWIG. All Monte Carlos include a CDF detector simulation. On the left in Fig. 10, the comparison of the topcolor Z' to SM $t\bar{t}$ simulations illustrates that in this data sample we are sensitive to topcolor Z' up to a mass of roughly $600 \text{ GeV}/c^2$. Finally, on the right in Fig. 10, we present the $t\bar{t}$ candidate mass distribution from CDF compared to the total standard model prediction. Given the statistics the agreement is quite good overall. The small shoulder of 6 events on a background of 2.4 in the region $475 < M < 550 \text{ GeV}/c^2$ is in an interesting mass region, given the dijet and $b\bar{b}$ search results, but is not statistically significant. Upper limits on the $t\bar{t}$ cross section as a function of $t\bar{t}$ mass, and on a topcolor Z' , are currently in progress.

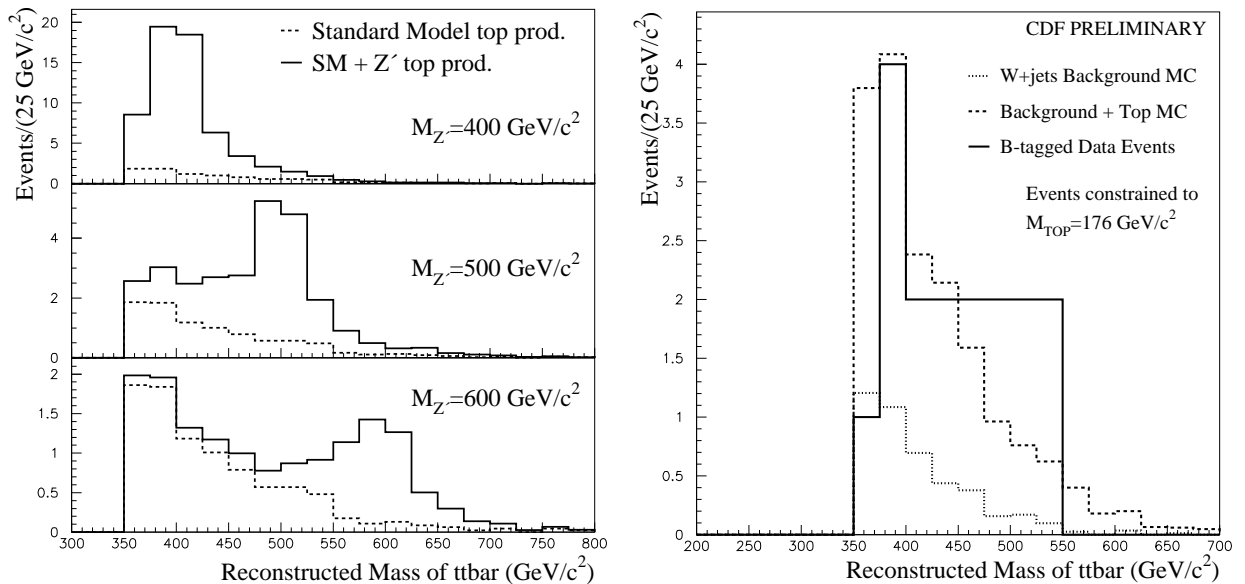


FIG. 10. left: Simulation of SM $t\bar{t}$ candidates (dashes) compared to SM + topcolor Z' (solid) for 3 different Z' masses. right: $t\bar{t}$ candidate data (solid) compared to $W + \text{jets}$ background MC (dotted) and total standard model background including $t\bar{t}$ (dashed). The simulations and data are for 67 pb^{-1} .

V. CONCLUSIONS

We have searched for new particles decaying to dijets, $b\bar{b}$, and $t\bar{t}$. In the dijet channel we set the most significant direct mass exclusions to date on the hadronic decays of axigluons (excluding $M < 1000$ GeV/c²), excited quarks (excluding $M < 600$ GeV/c²), technirhos (excluding $270 < M < 510$ GeV/c²), W' (excluding $380 < M < 470$ GeV/c²), Z' (excluding $410 < M < 460$ GeV/c²), and for the first time E6 diquarks (excluding $370 < M < 460$ GeV/c²). In the $b\bar{b}$ channel we set the first limits on topcolor, excluding a model of topgluons for width $\Gamma = 0.11M$ in the mass region $200 < M < 550$ GeV/c², $\Gamma = 0.3M$ for $210 < M < 450$ GeV/c², and $\Gamma = 0.5M$ for $200 < M < 370$ GeV/c². The search for topcolor in the $t\bar{t}$ channel has just begun and limits are in progress.

Limits are only a consolation prize; the main emphasis of our search is to explore the possibility of a signal. Although we do not have significant evidence for new particle production, the 500 – 600 GeV/c² region shows upward fluctuations in all three channels. We cannot ignore the exciting possibility that these apparently separate fluctuations may be the first signs of a new physics beyond the standard model. The remaining integrated luminosity for run 1B, currently being accumulated and analyzed, has the potential to either kill the fluctuations or reveal what may be the most interesting new physics in a generation.

REFERENCES

1. F. Abe et al. (CDF), Phys. Rev. Lett. **74**, 3538 (1995).
2. P. Frampton and S. Glashow, Phys. Lett. **B190**, 157 (1987).
3. U. Baur et al., Int. J. Mod. Phys A2, 1285(1987) & PRD**42**, 815(1990).
4. K. Lane et al., PRD**44**, 2768(1991) & Phys. Lett. **B327**, 129(1994).
5. J. Hewett and T. Rizzo, Phys. Rep. **183**, 193 (1989).
6. Talk by Anwar Bhatti in these proceedings.
7. Parameterization $d\sigma/dm = A(1 - m/\sqrt{s})^N/m^P$ with parameters A, N and P.
8. For new gauge bosons we use a K-factor to account for higher order terms.
9. J. Botts et al. (CTEQ Collaboration) Phys. Lett. **B304**, 159 (1993).
10. C. Hill and S. Parke, Phys. Rev. **D49**, 4454 (1994).
11. C. Hill, Phys. Lett. **B345**, 483 (1994).
12. F. Abe et al. (CDF), Phys. Rev. **D50**, 2966 (1994).
13. F. Abe et al. (CDF), Phys. Rev. Lett. **74**, 2626 (1995).
14. We model the interference between normal gluons and topgluons using hybrid model C in Phys. Rev. **D49**, 4454 (1994).
15. G. Burdman, C. Hill, and S. Parke private communication.